Sub Topic: Laminar Flames

10th U. S. National Combustion Meeting
Organized by the Eastern States Section of the Combustion Institute
April 23-26, 2017
College Park, Maryland

Effect of Surface Conditions on Fast Flame Acceleration in Obstructed Cylindrical Pipes

*Abdulafeez Adebiyi[1], Damir Valiev[2], V'yacheslav Akkerman[1,]**

[1]Center for Innovation in Gas Research and Utilization (CIGRU)
Center for Alternative Fuels, Engines and Emissions (CAFEE),
Computational Fluid Dynamics and Applied Multi-Physics Center (CFD&AMP)
Department of Mechanical and Aerospace Engineering, West Virginia University
Morgantown, WV 26506-6106, USA

[2]Center for Combustion Energy, Tsinghua University, Beijing, China

**Corresponding Author Email: Vyacheslav.Akkerman@mail.wvu.edu*

Abstract: The Bychkov model of extremely fast flame acceleration in obstructed pipes [Combust. Flame 157 (2010) 2012] employs a number of simplifying assumptions, including those of slip and adiabatic surfaces of the obstacles and of the pipe wall. In the present work, the influence of various mechanistic surface conditions on the flame dynamics in a cylindrical pipe of radius R, involving an array of parallel, tightly-spaced obstacles of length αR, is scrutinized by means of the computational simulations of the fully-compressible axisymmetric hydrodynamic and combustion equations with Arrhenius chemistry. Specifically, nonslip and slip surfaces are compared for the blockage ratio, α, and the spacing between the obstacles, Δz, in the ranges $1/3 \le \alpha \le 2/3$ and $0.25 \le \Delta z/R \le 2.0$, respectively. It is shown that the impact of surface friction on flame acceleration is minor, only 1.3~3.5%, being positive in a pipe with $\Delta z/R = 0.5$ and negative for $\Delta z/R = 0.25$. We have also demonstrated a minor effect of the isothermal surfaces as compared to the adiabatic ones [Phys. Fluids 28 (2016) 093602]. With the fact that the real boundary conditions are neither slip nor nonslip; neither adiabatic nor isothermal, but in between these categories, the present work thereby justifies the Bychkov model and makes its wider applicable to the practical reality. While this result can be anticipated and explained by the fact that the flame dynamics is mainly driven by its spreading in the unobstructed portion of an obstructed pipe (i.e. far from the wall), the situation is, however, qualitatively different from that in the unobstructed pipes, where the mechanistic and thermal wall conditions modify the flame dynamics conceptually.

Keywords: computational simulations, obstructed pipes; wall friction; boundary condition.

1. Introduction

Among the geometries associated with fast flame acceleration and the deflagration-to-detonation transition (DDT) scenarios, obstructed cylindrical pipes provide fastest acceleration [1]. While flame propagation through obstacles is oftentimes associated with turbulence/shocks [2], or hydraulic resistance [3], Bychkov *et al.* [4-7] have identified a conceptually laminar, shockless mechanism of ultrafast acceleration in semi-open channels or cylindrical tubes equipped with a comb-shaped array of obstacles. This mechanism is illustrated in Fig. 1, and it is devoted to a powerful jet-flow along the channel centerline, generated by a cumulative effect of delayed combustion in the "pockets" between the obstacles. According to the analytical formulation [5],

substantiated by the comprehensive computational simulations, a flame accelerates exponentially as $U_{tip}/S_L \approx \Theta\exp(\sigma\tau)$, where $U_{tip} \equiv dZ_{tip}/dt$ is the velocity of the flame tip in the laboratory reference frame, S_L the planar flame speed, $\Theta = \rho_u/\rho_b$ the thermal expansion ratio; $\tau = t\,S_L/R$ the scaled time, R the pipe radius, and the scaled exponential acceleration rate σ is given by [5]

$$\sigma = \sigma(\Theta,\alpha) = 2\frac{(\Theta-1)}{(1-\alpha)}\left[1+\frac{1}{2(\Theta-1)}\right], \qquad (1)$$

where α is the blockage ratio. This acceleration is extremely powerful indeed. Say, for typical $\Theta = 8$ and $\alpha = 1/2$, the quantity of σ is as large as 30! Moreover, σ grows with α and Θ, thereby promoting flame acceleration; it drastically depends on α; but it does not depend on R, which makes the Bychkov acceleration mechanism scale-invariant (Reynolds-independent) and, thus, relevant to various scales, from micro-combustors to very large mining and subway tunnels.

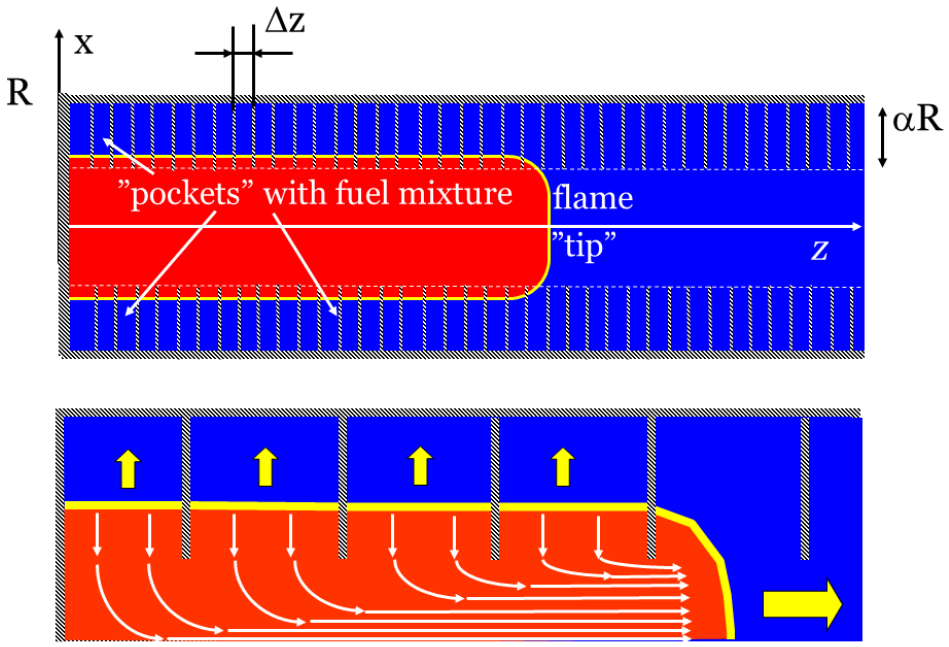

Figure 1: An illustration of the Bychkov mechanism of ultrafast flame acceleration in an obstructed pipe.

The theory and modelling [4-7] adopted a set of simplifications, such as adiabatic and freely-slip walls. With a fact that the real boundary conditions are neither slip nor nonslip; neither adiabatic nor isothermal, but in between these categories, the Bychkov model needed to be validated in terms of its applicability to the practical reality. Indeed, it was shown that both mechanistic and thermal (cold as well hot) wall boundary conditions play an enormous role in *unobstructed* pipes. Will it be the case for obstructed ones? Here we are answering this question. While Ugarte *et al.* [7] have recently shown a minor effect of the isothermal walls as compared to the adiabatic ones, in this work we have compared adiabatic and isothermal walls and came to the same conclusion.

2. Numerical Methods

We performed the computational simulations of the hydrodynamic and combustion equations including transport processes (thermal conduction, diffusion, and viscosity), full compressibility and an Arrhenius chemical kinetics. The basic equations in the cylindrical geometry read

$$\frac{\partial \rho}{\partial t}+\frac{1}{r}\frac{\partial}{\partial r}(r\rho u_r)+\frac{\partial}{\partial z}(\rho u_z)=0, \tag{2}$$

$$\frac{\partial}{\partial t}(\rho u_r)+\frac{\partial}{\partial z}(\rho u_z u_r-\zeta_{zr})+\frac{1}{r}\frac{\partial}{\partial r}\left[r\left(\rho u_r^2-\zeta_{rr}\right)\right]+\frac{\partial P}{\partial r}+\frac{1}{r}\zeta_{\theta\theta}=0, \tag{3}$$

$$\frac{\partial}{\partial t}(\rho u_z)+\frac{\partial}{\partial z}\left(\rho u_z^2-\zeta_{zz}\right)+\frac{1}{r}\frac{\partial}{\partial r}\left[r(\rho u_z u_r-\zeta_{zr})\right]+\frac{\partial P}{\partial z}=0, \tag{4}$$

$$\frac{\partial \varepsilon}{\partial t}+\frac{\partial}{\partial z}\left[(\varepsilon+P)u_z-\zeta_{zz}u_z-\zeta_{zr}u_r+q_z\right]+\frac{1}{r}\frac{\partial}{\partial r}\left[r\left((\varepsilon+P)u_r-\zeta_{rr}u_r-\zeta_{zr}u_z+q_r\right)\right]=0, \tag{5}$$

$$\frac{\partial}{\partial t}(\rho Y)+\frac{1}{r}\frac{\partial}{\partial r}\left(r\rho u_r Y-r\frac{\mu}{\mathrm{Sc}}\frac{\partial Y}{\partial r}\right)+\frac{\partial}{\partial z}\left(\rho u_z Y-\frac{\mu}{Sc}\frac{\partial Y}{\partial z}\right)=-\frac{\rho Y}{\tau_R}\exp\left(-E_a/R_u T\right), \tag{6}$$

where $\varepsilon=\rho(QY+c_P T)+\rho(u_z^2+u_r^2)/2$ is the total energy per unit volume and Y the mass fraction of the fuel mixture. The ideal gas model is used, such that $P=\rho R_u T/m$, $c_V=5R_u/2m$, $c_P=7R_p/2m$, with the adiabatic index $\gamma=c_P/c_V=1.4$, the molar mass $m=2.9\times10^{-2}$ kg/mol, and the universal gas constant $R_u=8.31\,\mathrm{J/(mol\cdot K)}$. The stress tensor $\zeta_{\alpha\beta}$ is given by

$$\zeta_{rr}=\mu\left(\frac{4}{3}\frac{\partial u_r}{\partial r}-\frac{2}{3}\frac{\partial u_z}{\partial z}-\frac{2}{3}\frac{u_r}{r}\right), \qquad \zeta_{zz}=\mu\left(\frac{4}{3}\frac{\partial u_z}{\partial z}-\frac{2}{3}\frac{\partial u_r}{\partial r}-\frac{2}{3}\frac{u_r}{r}\right), \tag{7}$$

$$\zeta_{\theta\theta}=\mu\left(\frac{4}{3}\frac{u_r}{r}-\frac{2}{3}\frac{\partial u_z}{\partial z}-\frac{2}{3}\frac{\partial u_r}{\partial r}\right), \qquad \zeta_{rz}=\mu\left(\frac{\partial u_z}{\partial r}+\frac{\partial u_r}{\partial z}\right), \tag{8}$$

and the energy diffusion vector q_α takes the form

$$q_r=-\mu\left(\frac{c_P}{\mathrm{Pr}}\frac{\partial T}{\partial r}+\frac{Q}{\mathrm{Sc}}\frac{\partial Y}{\partial r}\right), \qquad q_z=-\mu\left(\frac{c_P}{\mathrm{Pr}}\frac{\partial T}{\partial z}+\frac{Q}{\mathrm{Sc}}\frac{\partial Y}{\partial z}\right), \tag{9}$$

where $\mu\equiv\rho\nu$ is the dynamic viscosity, being $\mu_f=1.7\times10^{-5}\,kg/(\mathrm{m\cdot s})$ in the fuel mixture. Then the thermal flame thickness can be defined, conventionally, as $L_f=\mu_f\,\mathrm{Pr}\,\rho_f S_L=4.22\times10^{5}\,\mathrm{m}$.

A flame propagates in a long cylindrical pipe of radius R, with one end open, and with an unobstructed central portion, of radius $(1-\alpha)R$, while the rest is blocked by the obstacles with the spacing (the distance between two neighboring obstacles) ΔZ, see Fig. 1. This geometry is described by the flame propagation Reynolds number $\mathrm{Re}\equiv RS_L/\nu=R/\mathrm{Pr}\,L_f=R/L_f$. In the present work we used $\Delta Z/R=1/4$, 1/2 and 2.0; Re = 12 and 24; and $\alpha=1/3;1/2;2/3$. We considered adiabatic ($\mathbf{n}\cdot\nabla T=0$) and either free-slip ($\mathbf{n}\cdot\mathbf{u}=0$) or non-slip ($\mathbf{u}=0$) surfaces of the obstacles and of the pipe wall, where $\mathbf{n}$ is a normal vector at a surface. The absorbing (non-reflecting) boundary conditions are employed at the open end to prevent the reflection of the sound waves and weak shocks. The left end of the free part of the channel is blocked, while the other end, on the right, is open, with the boundary conditions $\rho=\rho_f$, $P=P_f$, $u_z=0$ adopted. The initial flame structure was imitated by the classical Zeldovich-Frank-Kamenetsky (ZFK) solution for a hemispherical flame front [7] ignited at the centerline, at the closed end of the pipe.

3. Results and Discussion

We have compared the cases of freely-slip and non-slip boundary conditions, quantitatively, by the plots of Figs. 2-6, and qualitatively, by the snapshots of Figs. 7-8, for various R, ΔZ, and α.

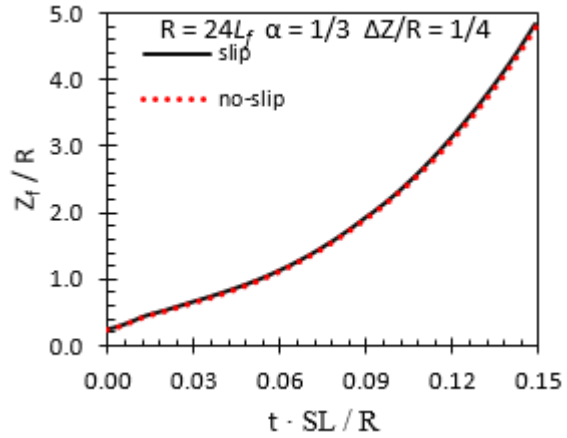

Figure 2: The scaled flame position Z_f / R vs the scaled time τ for R = 24L_f, α = 1/3 and ΔZ/R = 1/4.

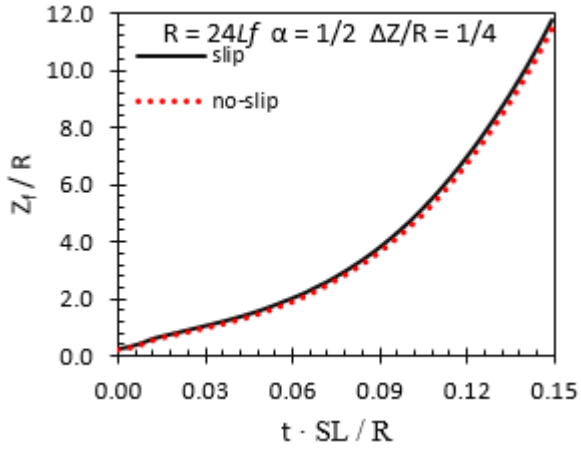

Figure 3: The scaled flame position Z_f / R vs the scaled time τ for R = 24L_f, α = 1/2 and ΔZ/R = 1/4.

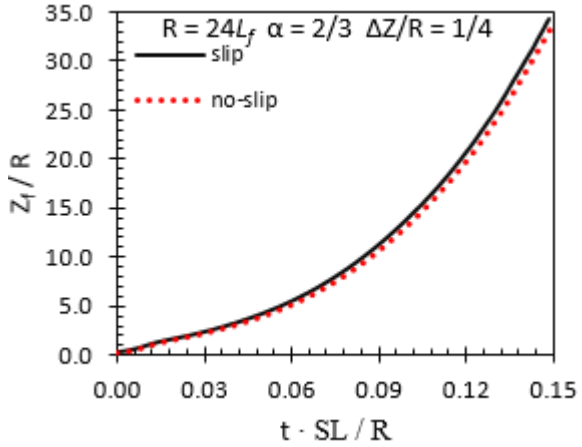

Figure 4: The scaled flame position Z_f / R vs the scaled time τ for R = 24L_f, α = 2/3 and ΔZ/R = 1/4.

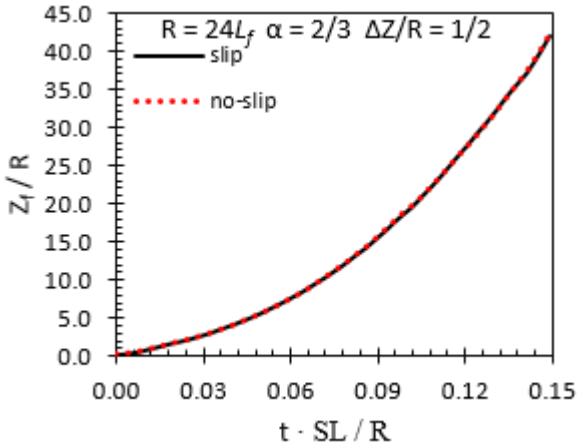

Figure 5: The scaled flame position Z_f / R vs the scaled time τ for R = 24L_f, α = 2/3 and ΔZ/R = 1/2.

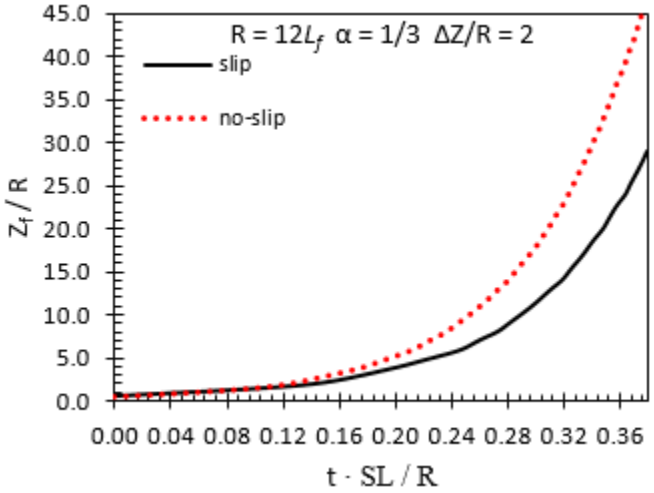

Figure 6: The scaled flame position Z_f / R vs the scaled time τ for R = 12L_f, α = 1/3 and ΔZ/R = 2.

Specifically, the scaled flame tip position Z_f / R versus the scaled time $\tau = t S_L / R$ is presented in Figs. 2-6, with the free-slip and non-slip boundary conditions shown by the solid black and the dashed red lines, respectively, in all the plots. It is seen that that the effect of mechanistic surface boundary conditions is minor as long as the obstacles spacing is small, $\Delta Z \le R/2$, and this is true for all α considered. Indeed, both the curves almost coincide in Figs. 2, 3 and 5, and the difference between them is hardly seen and in Fig. 4. A reasonable way the measure a relative deviation between the plots is the quantity (in %):

$$E = \left| (Z_{f,slip} - Z_{f,no-slip}) / Z_{f,no-slip} \right| \times 100 . \qquad (10)$$

The result (10) does not exceed 3.1~3.5 % for all the cases depicted in Figs. 2-5; friction slightly moderates flame acceleration for $\Delta Z = R/4$, and very slightly promotes it for $\Delta Z = R/2$. This result certifies a minor impact of the mechanistic boundary conditions and thereby justifies the Bychkov model of flame acceleration in obstructed pipes, which employs the freely-slip obstacles and walls. This result can be explained by the fact that the flow is mainly driven in the axial direction such that the small obstacle spacing mitigates a potential effect of wall fiction (if any). In fact, Ref. [7] recently suggested the same conclusion with the same explanation when studying the thermal boundary conditions at the walls and obstacles in obstructed channels.

However, the situation differs noticeably for larger obstacles spacing as clearly seen in Fig. 6, for $\Delta Z = 2R$. Here, wall friction promotes flame acceleration, substantially, as compared to the slip conditions. The deviation (10) is as large as 24% in that case. Such a discrepancy can be devoted to the formation of vorticity (or even turbulence) in the pockets between the obstacles in this configuration. Obviously, vorticity evolves differently with slip and non-slip walls, with a stronger flow distortion in the latter case, leading thereby to faster flame acceleration. It is noted that the Bychkov model does not consider vorticity, and hence it is probably not applicable here. Moreover, the very approach of tightly-spaced obstacles, $\Delta Z << R$, Fig. 1, is broken when ΔZ exceeds R. In fact, an inapplicability of the Bychkov formulation for $\Delta Z > R$ was shown even in the pilot study [5] and later in the detailed analysis [7]. Hence, our work agrees with Refs. [5,7].

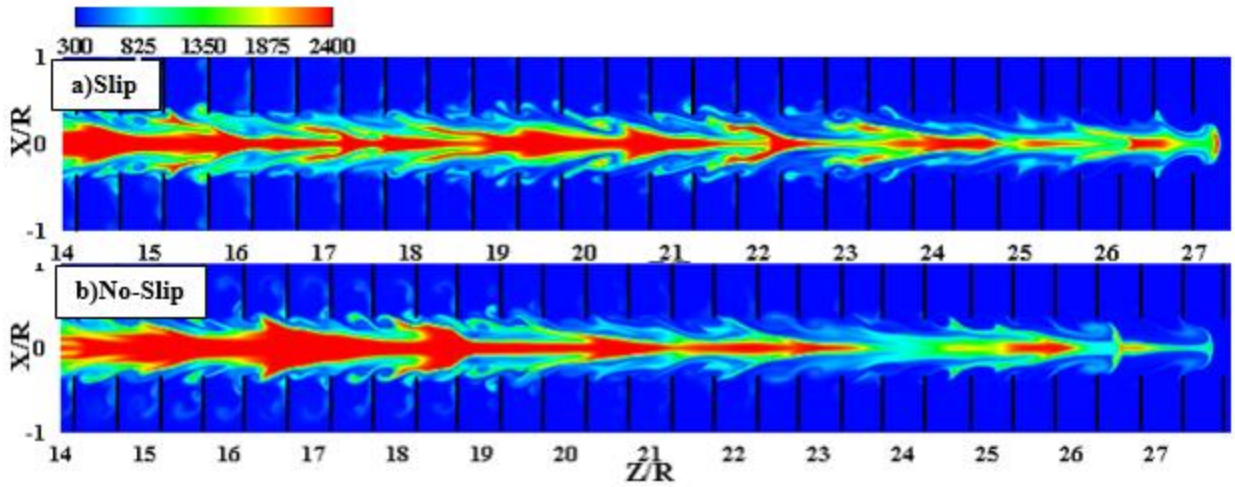

Figure 7: The flame evolution in tube of R = 24L_f α = 2/3 and ΔZ/R = 1/2: **a)** slip and **b)** noslip.

Qualitatively, we arrive to the same conclusions by means of the color snapshots in Figs.7-8. Specifically, Fig. 7 compares the flame shape and position for $\Delta Z = R/2$ taken at the same time instant, $\tau = 0.15$, for slip (a) and non-slip (b) cases. A resemblance between Figs. 7a and 7b is

evident, with the flame positioned at $Z_f \sim 27R$ in both figures. Figure 8 is a counterpart of Fig. 7 for $\Delta Z = 2R$, $\tau = 0.38$. Unlike Fig. 7, the discrepancy between Figs. 8a and 8b is clearly seen.

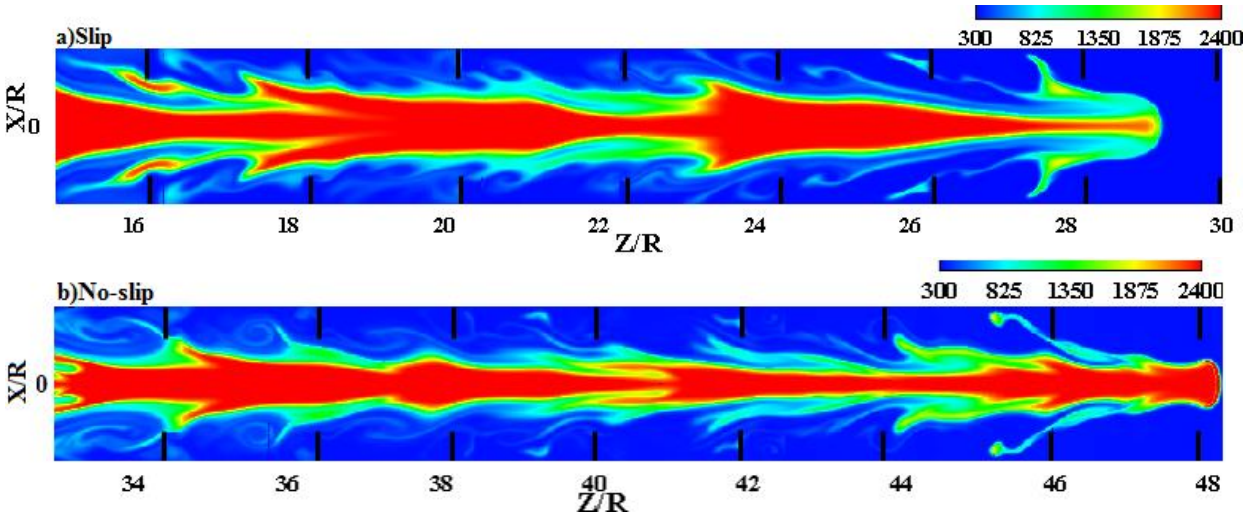

Figure 8: The flame evolution tube of R= $12L_f$ R = $12L_f$ α = 1/3 and ΔZ/R = 2.0 **a)**slip **b)**No-slip walls

4. Conclusion

We have investigated flame propagation in obstructed cylindrical pipes. It is shown that an impact of surface friction on flame acceleration is minor, 1.3~3.5%, being positive in a pipe with $\Delta Z = R/2$ and negative for $\Delta Z = R/4$. We also demonstrated a minor effect of the isothermal surfaces as compared to the adiabatic ones [7]. With the fact that the real boundary conditions are neither slip nor nonslip; neither adiabatic nor isothermal, but in between these categories, the present work thereby justifies the Bychkov model and makes its wider applicable to the practical reality. While this result can be anticipated and explained by the fact that the flame dynamics if mainly driven by its spreading in the unobstructed portion of an obstructed pipe (i.e. far from the wall), the situation is, however, qualitatively different from that in the unobstructed pipes, where the mechanistic and thermal wall conditions modify the flame dynamics conceptually.

5. Acknowledgements

This work is supported by the National Science Foundation (NSF) through the CAREER Award No. 1554254 (V.A.).

6. References

[1] E.S. Oran, V.N. Gamezo, Origins of the deflagration-to-detonation transition in gas-phase combustion, Combustion and Flame 148 (2007) 4-47.
[2] G. Ciccarelli, S. Dorofeev, Flame acceleration and transition to detonation in ducts, Progress in Energy and Combustion Science 34 (2008) 499-550.
[3] I. Brailovsky, L. Kagan, G. Sivashinsky, Combustion waves in hydraulically resisted systems, Phil. Trans. R. Soc. A 370 (2012) 625-646.
[4] V. Bychkov, D. Valiev, L.-E. Eriksson, Physical mechanism of ultrafast flame acceleration, Physical review letters 101 (2008) 164501.
[5] D. Valiev, V. Bychkov, V. Akkerman, C.K. Law, L.-E. Eriksson, Flame acceleration in channels with obstacles in the deflagration-to-detonation transition, Combustion and Flame 157 (2010) 1012-1021.
[6] V. Bychkov, V. Akkerman, D. Valiev, C.K. Law, Influence of gas compression on flame acceleration in channels with obstacles, Combustion and Flame 157 (2010) 2008-2011.
[7] O. Ugarte, V. Bychkov, J. Sadek, D. Valiev, V. Akkerman, Critical role of blockage ratio for flame acceleration in channels with tightly spaced obstacles, Physics of Fluids 28 (2016) 093602.